

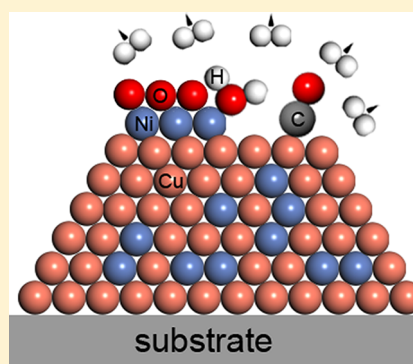
Inverse NiO_{1-x}/Cu Catalyst with High Activity toward Water–Gas Shift

Li-Yong Gan and Yu-Jun Zhao*

Department of Physics, South China University of Technology, and Key Laboratory of Clean Energy Materials of Guangdong Higher Education Institute, Guangzhou 510640, P. R. China

S Supporting Information

ABSTRACT: Ni additives into Cu catalyst can enhance the activity to the water–gas shift (WGS) reaction. However, an undesirable side reaction (methanation) would arise synchronously, consequently sharply degrading the selectivity to WGS. Herein, we propose an improved CuNi model system with potential excellent performance (both activity and selectivity) toward WGS, i.e., the inverse NiO_{1-x}/Cu(111) ($x < 1$). The unsaturated Ni^{δ+} species are expected to facilitate the rate-limiting step of WGS remarkably, H₂O dissociation, and subsequently, a rather smooth potential energy surface is found in the rest of the steps of WGS over the interface of NiO_{1-x}/Cu(111), indicating a high reactivity. Meanwhile, a weak interaction between CO and NiO_{1-x} and a low activity of NiO_{1-x}/Cu(111) toward CO dissociation imply that the oxidized Ni^{δ+} species can effectively suppress the undesirable methanation found in CuNi catalysts, expecting to improve its selectivity toward WGS. The model system may be also applied to catalyze CO oxidation at proper conditions.



The water–gas shift (WGS) reaction, $\text{CO} + \text{H}_2\text{O} \leftrightarrow \text{CO}_2 + \text{H}_2$, is an important chemical process for maximizing hydrogen production and removing residual CO in H₂ fuel cell systems and thus attracts increasingly interest in heterogeneous catalysis.¹ Current industrial employed WGS catalysts are based on a two-step reactor: high-temperature shift (Fe₂O₃/Cr₂O₄) and low-temperature shift (Cu/ZnO/Al₂O₃).² For the copper-based WGS catalysts, H₂O dissociation is found to be the rate-limiting step for the entire WGS process.³ In order to explore highly active WGS catalysts, considerable studies have been carried out by both experiments and theoretical calculations on a series of model catalysts including pure metal surfaces,^{3,4} bimetallic surfaces,^{5–7} metallic nanoparticles supported on oxide surfaces,^{8,9} and inverse oxide nanoparticles supported on metal surfaces.^{10,11} Researchers, however, still hike on the way of pursuing highly efficient WGS catalysts.

A recent study showed that the bimetallic CuNi catalysts demonstrate a better activity to WGS reaction relative to the pure Cu. However, the Ni additives in the Cu catalysts could also enhance an undesirable side-reaction (methanation) synchronously,⁶ namely, the selectivity to WGS degrades. Then, how do we overcome this drawback? Inspired by a recent work of WGS on oxide/Cu(111),¹² we herein propose an improved CuNi model system, i.e., the inverse NiO_{1-x}/Cu(111) ($x < 1$) aiming for a high performance including both activity and selectivity toward WGS. Namely, a rather smooth reaction potential energy surface of WGS on NiO_{1-x}/Cu indicates a high reactivity, while the low activity of NiO_{1-x}/Cu(111) toward CO dissociation (both direct and indirect) implies that the model system would effectively suppress the undesirable methanation found in CuNi catalysts, expecting to improve its selectivity toward WGS. Around the interface of

this system, multiple sites (unsaturated Ni^{δ+} cations, as well as O^{δ-} anions and Cu atoms nearby) can be provided for the WGS process according to a bifunctional mechanism.^{10,13}

The state-of-the-art density functional theory¹⁴ (DFT) has been proved to be such a powerful and effective tool, which will enable us to understand heterogeneous catalysis at a molecular level,¹⁵ and even design new model catalysts with high performance.^{13,16} In the present work, we perform DFT calculations¹⁴ to manifest the catalytic performance of the inverse NiO_{1-x}/Cu(111) toward WGS. The computational details can be found in the Supporting Information.

To model NiO_{1-x} nanoparticles supported on Cu(111), a chain of NiO nanoparticles are deposited on Cu(111), similar to what Liu proposed for oxide/Cu systems.¹² After fully structural relaxing, a wave-like periodic chain of NiO_{1-x} is obtained, as shown in Figure S1a,b, Supporting Information. A remarkable distortion can be seen in the surface layer due to the strong interactions between NiO_{1-x} and Cu(111), giving rise to an energy cost of 0.40 eV relative to the clean Cu(111). To estimate the stability of this nanostructure, the binding energy (E_b) of the chain on the corrugated surface is calculated as $E_b = E_{\text{NiO}_{1-x}/\text{Cu}(111)} - E_{\text{Cu}(111)} - 3E_{\text{NiO-bulk}} - E_{\text{NiO}_{1-x}/\text{Cu}(111)}$, and $E_{\text{Cu}(111)}$ are the total energies of the NiO_{1-x}/Cu(111) and corrugated Cu(111) surface, respectively. $E_{\text{NiO-bulk}}$ is the bulk energy per NiO formula in its antiferromagnetic ground state.¹⁷ The factor 3 to the $E_{\text{NiO-bulk}}$ indicates there are three NiO formulas in the chain structure. The binding energy is negative

Received: April 27, 2012

Revised: June 20, 2012

Published: July 9, 2012

(−1.42 eV) with respect to the bulk NiO, indicating that NiO prefers to bind on Cu(111) and form nanoparticles rather than to aggregate into larger particles. These results are very similar to that in the NiO_{1-x}/Pt(111) system,¹⁸ which demonstrated that the formed NiO_{1-x} are highly dispersed on the Pt(111) surface. Of note, the calculated Ni–O bond length (1.79 Å) in the chain is substantially shortened with respect to that in the bulk NiO, 2.09 Å.

Subsequently, the WGS process is investigated on NiO_{1-x}/Cu(111). A feasible pathway is identified, following the mechanism: H₂O* → H* + OH*; CO* + OH* → COOH* + H*; COOH* → CO₂* + H*; H* + H* → H₂. The transition states (TS) of the first three elementary steps are calculated by the climbing-image nudged elastic band (CI-NEB),¹⁹ and the reaction barriers are determined. For comparison, the WGS process via the more reasonable COOH-mediated mechanism³ is also studied on Cu(111) and CuNi(111) with nonadjacent Ni pairs incorporated in the surface layer [cf. Figure S1c, Supporting Information]. The reaction potential energy surfaces (PES) are summarized in Figure 1, and the optimized structures at each step of the WGS are shown in Figure S2, Supporting Information.

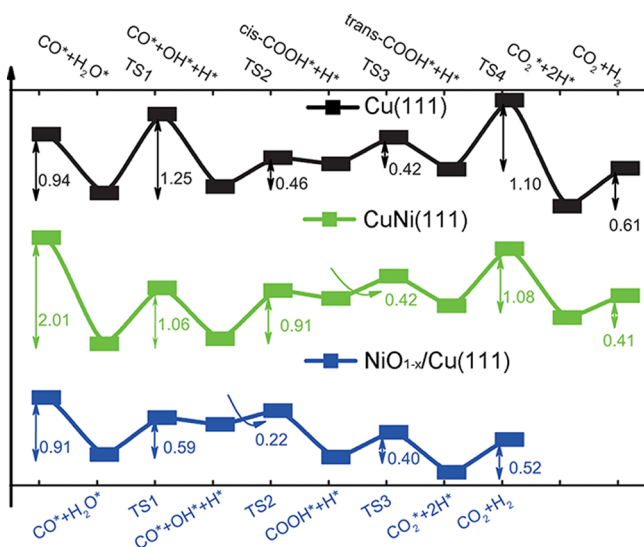


Figure 1. Potential energy surfaces (PES) for WGS on Cu(111) (black curve and fonts), CuNi(111) (green curve and fonts), and the inverse NiO_{1-x}/Cu(111) (blue curve and fonts). The corresponding optimized structures for different steps in WGS on the three surfaces are shown in Figure S2, Supporting Information

Let us first consider the WGS reaction, following the COOH-mediated mechanism, on the CuNi(111) bimetallic surface with respect to the benchmark Cu(111) surface. The most energetically favorable adsorption site for both H₂O and CO on CuNi(111) surface is the top of the Ni atom, so the configuration with H₂O and CO coadsorption on two atop sites of Ni was selected as the starting point of the whole WGS reaction [cf. the coadsorption of CO and H₂O configuration on CuNi(111) in Figure S2, Supporting Information]. From the PES (cf. Figure 1), one can see that introducing Ni atoms into the Cu catalyst is able to lower the barrier of the first step of WGS, the partial dissociation of adsorbed water. In the second step, the barrier of CO oxidation by OH increases because CO adsorption is strengthened on the top of the Ni monomer.⁷ In the rest of the three processes, the PES on the CuNi(111) is

found to be similar to that on Cu(111). Since H abstraction from H₂O dissociation on Cu catalyst is the bottleneck of the entire WGS process, it is expected that lowering its barrier by Ni additives can eventually enhance the reactivity toward WGS as observed experimentally.⁶ However, the promotion of Ni additives in the Cu catalyst may be somewhat limited. In addition, the interaction of Ni–CO is much stronger than that of Cu–CO on the CuNi surface. The most energetically favorable adsorption site for CO on CuNi(111) is the top of the Ni atom, and moreover, our previous study⁷ showed that the binding of CO is strengthened from −1.66 eV on Ni monomer through −1.89 eV on Ni dimer to −2.14 eV on Ni trimer. Such favorable Ni–CO interaction infers that CO adsorption on the CuNi bimetallic surface may result in thermodynamic aggregation of Ni atoms. If the Ni concentration increases, the process would be further accelerated, and ultimately favor the methanation instead of the oxidation of CO.⁶ Additionally, we also studied the H₂O partial dissociation and CO oxidation by OH on the CuNi bimetallic surface with a Ni monolayer in the subsurface layer to investigate the effects of subsurface Ni atoms on WGS. The calculated reaction barriers are 1.24 and 0.46 eV, respectively, suggesting that the subsurface Ni atoms have tiny effects on the reactivity toward WGS. Fortunately, as discussed below, the formed oxidized Ni structures may overcome the drawbacks of CuNi catalyst and thus show excellent performance toward WGS.

Over NiO_{1-x}/Cu(111), the entire process starts from the coadsorption of the two reactants at their respective most energetically favorable site, H₂O on Ni^{δ+} and CO on Cu atom with an energy gain of 0.91 eV. Then, the H₂O molecule dissociates to produce OH and H with a modest reaction barrier of 0.59 eV. Subsequently, the dissociated OH can readily react with the adsorbed CO nearby, overcoming a fairly small barrier (0.22 eV) to yield a COOH entity. This smooth step is exothermically favorable by 0.52 eV. The carboxyl species decomposes into an adsorbed H atom and CO₂ (exothermic by 0.24 eV), passing an activation barrier of 0.40 eV. Finally, the two adsorbed H atoms combine with each other to form an H₂ molecule. This step is endothermic by 0.52 eV. The recombination of H₂ can be facilitated by a large entropy at elevated temperatures,⁸ and therefore, we did not consider its pathway. Generally, it can be seen that the H₂O adsorption and partial dissociation steps occur on NiO_{1-x} while CO adsorbs at those sites on a Cu substrate nearby, the so-called bifunctional mechanism.^{10,13} Furthermore, it can be noticed that the subsequent steps of CO oxidation and the production of H₂ take place at the boundary of NiO_{1-x}/Cu(111), indicating a crucial role of the interface in the process of WGS.

Our calculations demonstrate that the reactivity toward WGS on the inversed NiO_{1-x}/Cu(111) could be much higher than that on the benchmark surface of Cu(111) as well as the bimetallic CuNi(111). First, the water dissociation step, which is the bottleneck of the entire WGS process on clean Cu(111), is much more facile, 0.59 eV vs 1.25 eV. The value is also much smaller than that on CuNi bimetallic surface, 1.06 eV. The pathway of CO oxidation with the dissociated OH is still as smooth as that on Cu, and much lower than that on CuNi. Additionally, the reaction barrier of COOH dissociation into CO₂ and H atom on NiO_{1-x}/Cu(111) is nearly one-third of the value on the Cu(111) surface, 0.40 vs 1.10 eV. The value is even smaller than that on the catalyst of gold nanoparticles supported on a reduced CeO₂(111).⁸ The two low barriers of H abstraction from water and carboxyl may be attributed to the

O-assisted O–H bond splitting.²⁰ It was reported that the presence of O adatoms on a serial of transition metal surfaces could lower both the reaction energies and reaction barriers of O–H bonds cleavage, and the O-induced promotion effect was found linearly dependent on the O adsorption energy. That is, the more strongly the oxygen atoms bind to the metal surface, the less promoting effect they have on the water O–H bond splitting. This may result from the different degree of unsaturation of O on those surfaces: the lower adsorption energy of O, the higher the degree of unsaturation of O atom. In NiO_{1-x}, O atoms are highly unsaturated, and similar promotion effects on O–H bond cleavage could be expected.

CO adsorption on the NiO_{1-x} chain with a number of configurations and both the direct CO dissociation and the indirect dissociation assisted by an H atom are calculated to probe the activity of the model catalyst toward CO methanation. It is found that CO adsorption on the top of Ni is more favorable with a binding energy of -0.59 eV. However, the absolute value is still smaller than that on a Cu site (-0.76 eV).⁷ The weaker adsorption of CO on Ni is actually similar to the case of CO adsorption on the O precovered Ni metallic surface and can be understood by the d-band model.²¹ As for CO dissociation, we first consider the direct dissociation. It was found that the process must overcome a rather high reaction barrier (3.84 eV) on the Cu surface if the reaction center is away from NiO_{1-x}, while the reaction energy is as high as 5.12 eV if the center is over the interface of NiO_{1-x}/Cu(111), and thus, we did not calculate the reaction pathway. These values indicate that it is extremely unfavorable for CO direct dissociation on NiO_{1-x}/Cu(111). In the indirect path, we first performed the adsorption calculation of CHO over the interface. However, CHO would dissociate spontaneously into CO and H during the structural relaxation. We did not consider CHO adsorption on those Cu atoms that are away from the interface since Cu was reported to be against CO methanation.⁶ These results undoubtedly verify that the NiO_{1-x}/Cu(111) system could lead to a low activity toward methanation, and namely, the selectivity toward WGS is high. Therefore, the partially oxidized Ni species (Ni^{δ+}) can effectively suppress the undesired methanation aroused by the Ni additives in CuNi bimetallic catalysts.⁶

In CuNi alloys, it is energetically favorable for Ni impurities to stay in the bulk to form particles with Cu-rich shells and Ni-rich cores.²² The energy difference between a Ni atom in the surface and subsurface layer under vacuum condition is 0.21 eV, while it becomes negative (-0.21 eV) with the subsurface Ni segregating out to bind to an O atom. This implies that Ni impurities tend to segregate out of the surface under oxidizing conditions due to the strong interaction between Ni and O. Therefore, a NiO_{1-x} nanostructure supported Cu catalyst can be readily prepared from the bimetallic CuNi under proper oxidizing condition (Figure S3, Supporting Information) or by depositing Ni on Cu(111) under oxidizing conditions as the preparations of FeO_{1-x}/Pt(111)¹³ and NiO_{1-x}/Pt(111).¹⁸ Meanwhile, a small amount of Cu^{δ+} may not be avoidable in surface area during the preparation. Fortunately, the presence of Cu^{δ+} (mainly in the form of Cu₂O) is also beneficial for inducing H₂O dissociation.²³ The Cu^{δ+} species would be reduced to Cu by CO during WGS.¹¹ The Ni^{δ+} may still exist in the reductive H₂ environment similar to FeO_{1-x}/Pt(111) and NiO_{1-x}/Pt(111) in CO PROX reaction (i.e., 1% CO and 0.5% O₂; 98.5% H₂)^{13,18} at proper operating temperature, hence remaining highly active to the water dissociation.

In summary, our theoretical study demonstrates that the inverse NiO_{1-x}/Cu(111) could be a promising catalyst toward WGS with excellent reactivity and selectivity. It shows that partially oxidized Ni^{δ+} species can remarkably facilitate the rate-limiting step of WGS, H₂O dissociation. Furthermore, a rather smooth potential energy surface is found in the rest of the steps of WGS over the interface of NiO_{1-x}/Cu(111). The system potentially makes full use of the bifunctional mechanism and implies a high reactivity to WGS. Meanwhile, a weak interaction between CO and NiO_{1-x} and a low activity of NiO_{1-x}/Cu(111) toward CO dissociation (both direct and indirect) indicate that the oxidized Ni^{δ+} species can effectively suppress the undesirable methanation found in CuNi catalysts, expecting to improve its selectivity toward WGS. Additionally, the system may be also applied to catalyze CO oxidation at low temperatures, similar to FeO/Pt(111).²⁴ The metal–oxide premiers facilitate water dissociation to form OH groups, which subsequently not only promote the activation of oxygen molecules but also open a more readily reaction channel for CO oxidation.

■ ASSOCIATED CONTENT

📄 Supporting Information

Model and computational details used in the present work and structural data and imaginary frequencies of transition states of WGS on Cu(111), CuNi(111), and NiO_{1-x}/CuNi(111) surfaces. This material is available free of charge via the Internet at <http://pubs.acs.org>.

■ AUTHOR INFORMATION

Corresponding Author

*Tel: +86-20-87110426. Fax: +86-20-87112837. E-mail: zhaoyj@scut.edu.cn.

Notes

The authors declare no competing financial interest.

■ ACKNOWLEDGMENTS

We wish to thank Professor Wei-Xue Li for the critical reading of the manuscript and valuable suggestions. This work is supported by MOST, under project 2010CB631302, and the Fundamental Research Funds for the Central Universities, SCUT, under projects 2011ZG0017 and 2011ZM0090, and completed with the cooperation of HPC Lab, Shenzhen Institute of Advanced Technology, CAS, China.

■ REFERENCES

- (1) Navarro, R. M.; Pena, M. A.; Fierro, J. L. G. *Chem. Rev.* **2007**, *107* (10), 3952–3991.
- (2) Ovesen, C. V.; Clausen, B. S.; Hammershøi, B. S.; Steffensen, G.; Askgaard, T.; Chorkendorff, I.; Nørskov, J. K.; Rasmussen, P. B.; Stoltz, P.; Taylor, P. J. *Catal.* **1996**, *158* (1), 170–180.
- (3) Gokhale, A. A.; Dumesic, J. A.; Mavrikakis, M. *J. Am. Chem. Soc.* **2008**, *130* (4), 1402–1414.
- (4) Grabow, L. C.; Gokhale, A. A.; Evans, S. T.; Dumesic, J. A.; Mavrikakis, M. *J. Phys. Chem. C* **2008**, *112* (12), 4608–4617. Fajin, J. L. C.; Cordeiro, M. N. D. S.; Illas, F.; Gomes, J. R. B. *J. Catal.* **2009**, *268* (1), 131–141. Huang, S.-C.; Lin, C.-H.; Wang, J. H. *J. Phys. Chem. C* **2010**, *114* (21), 9826–9834.
- (5) Knudsen, J.; Nilekar, A. U.; Vang, R. T.; Schnadt, J.; Kunkes, E. L.; Dumesic, J. A.; Mavrikakis, M.; Besenbacher, F. *J. Am. Chem. Soc.* **2007**, *129* (20), 6485–6490. Jelic, J.; Meyer, R. J. *J. Catal.* **2010**, *272* (1), 151–157. Huang, T. J.; Yu, T. C.; Jhao, S. Y. *Ind. Eng. Chem. Res.* **2006**, *45* (1), 150–156.

- (6) Lin, J. H.; Biswas, P.; Gulians, V. V.; Mixture, S. *Appl. Catal., A* **2010**, *387* (1–2), 87–94.
- (7) Gan, L.-Y.; Tian, R.-Y.; Yang, X.-B.; Lu, H.-D.; Zhao, Y.-J. *J. Phys. Chem. C* **2012**, *116* (1), 745–752.
- (8) Liu, Z.-P.; Jenkins, S. J.; King, D. A. *Phys. Rev. Lett.* **2005**, *94* (19), 196102.
- (9) Rodriguez, J. A.; Liu, P.; Wang, X.; Wen, W.; Hanson, J.; Hrbek, J.; Perez, M.; Evans, J. *Catal. Today* **2009**, *143* (1–2), 45–50. Fu, Q.; Saltsburg, H.; Flytzani-Stephanopoulos, M. *Science* **2003**, *301* (5635), 935–938.
- (10) Rodriguez, J. A.; Ma, S.; Liu, P.; Hrbek, J.; Evans, J.; Perez, M. *Science* **2007**, *318*, 1757–1760.
- (11) Rodriguez, J. A.; Graciani, J.; Evans, J.; Park, J. B.; Yang, F.; Stacchiola, D.; Senanayake, S. D.; Ma, S.; Perez, M.; Liu, P.; Fdez Sanz, J.; Hrbek, J. *Angew. Chem., Int. Ed.* **2009**, *48* (43), 8047–8050.
- (12) Fu, Q.; Li, W. X.; Yao, Y. X.; Liu, H. Y.; Su, H. Y.; Ma, D.; Gu, X. K.; Chen, L. M.; Wang, Z.; Zhang, H.; Wang, B.; Bao, X. H. *Science* **2010**, *328* (5982), 1141–1144.
- (13) Perdew, J. P.; Yue, W. *Phys. Rev. B* **1986**, *33* (12), 8800–8802. Perdew, J. P.; Chevary, J. A.; Vosko, S. H.; Jackson, K. A.; Pederson, M. R.; Singh, D. J.; Fiolhais, C. *Phys. Rev. B* **1992**, *46* (11), 6671–6687.
- (14) Honkala, K.; Hellman, A.; Remedakis, I. N.; Logadottir, A.; Carlsson, A.; Dahl, S.; Christensen, C. H.; Nørskov, J. K. *Science* **2005**, *307* (5709), 555–558.
- (15) Hellman, A.; Baerends, E. J.; Biczysko, M.; Bligaard, T.; Christensen, C. H.; Clary, D. C.; Dahl, S.; van Harrevelt, R.; Honkala, K.; Jonsson, H.; Kroes, G. J.; Luppi, M.; Manthe, U.; Nørskov, J. K.; Olsen, R. A.; Rossmeisl, J.; Skulason, E.; Tautermann, C. S.; Varandas, A. J. C.; Vincent, J. K. *J. Phys. Chem. B* **2006**, *110* (36), 17719–17735.
- (16) Liu, P. *J. Chem. Phys.* **2010**, *133* (20), 204705.
- (17) Zhang, W.-B.; Hu, Y.-L.; Han, K.-L.; Tang, B.-Y. *Phys. Rev. B* **2006**, *74* (5), 054421.
- (18) Mu, R. T.; Fu, Q. A.; Xu, H.; Zhang, H. I.; Huang, Y. Y.; Jiang, Z.; Zhang, S. O.; Tan, D. L.; Bao, X. H. *J. Am. Chem. Soc.* **2011**, *133* (6), 1978–1986.
- (19) Henkelman, G.; Uberuaga, B. P.; Jonsson, H. *J. Chem. Phys.* **2000**, *113* (22), 9901.
- (20) Wang, G.-C.; Tao, S.-X.; Bu, X.-H. *J. Catal.* **2006**, *244* (1), 10–16.
- (21) Hammer, B.; Nørskov, J. K. *Adv. Catal.* **2000**, *45*, 71–129 and references therein.
- (22) Ahmed, J.; Ramanujachary, K. V.; Lofland, S. E.; Furiato, A.; Gupta, G.; Shivaprasad, S. M.; Ganguli, A. K. *Colloids Surf., A* **2008**, *331* (3), 206–212.
- (23) Chen, C. S.; Chen, C. C.; Lai, T. W.; Wu, J. H.; Chen, C. H.; Lee, J. F. *J. Phys. Chem. C* **2011**, *115* (26), 12891–12900.
- (24) Gu, X.-K.; Ouyang, R.; Sun, D.; Su, H.-Y.; Li, W.-X. *ChemSusChem* **2012**, *5* (5), 871–878.